Electronic Supplementary Material (ESI) for Energy & Environmental Science.
This journal is © The Royal Society of Chemistry 2014

Electronic Supplementary Information

Surface termination and Subsurface Restructuring of Perovskite-based Solid Oxide Electrode Materials

John Druce [a,,+], Helena Téllez [b,‡,*,+], Mónica Burriel [b,§], Matthew D. Sharp [b], Lydia J. Fawcett [b], Stuart N. Cook [b,‖], David. S. McPhail [b], Tatsumi Ishihara [a], Hidde H. Brongersma [c], and John A. Kilner [a,b,*]*

[+] *These authors contributed equally to this work*

[a] *International Institute for Carbon Neutral Energy Research (wpi-I2CNER), Kyushu University, Nishi-ku, Fukuoka, 819-0395, JAPAN. Email: john.druce@i2cner.kyushu-u.ac.jp; htellez@i2cner.kyushu-u.ac.jp; j.kilner@imperial.ac.uk. Tel: +81(0)92-802-6738 (JD,HT); +44(0)207-594-6745 (JK).*

[b] *Department of Materials, Imperial College London, South Kensington, London, SW7 2AZ, UK.*

[c] *Department of Applied Physics, Eindhoven University of Technology, P.O. Box 513, 5600 MB Eindhoven, The Netherlands.*

‡ *Present affiliation: as (a)*

§ *Present affiliation: Department of Advanced Materials for Energy, Catalonia Institute for Energy Research (IREC), Adriá del Besòs, Barcelona, Spain*

‖ *Present affiliation: Department of Materials Science and Engineering, Massachusetts Institute of Technology, Cambridge, MA 02139, USA*

Sample preparation

The starting single-perovksite (LSCF-113) and Ruddlesden-Popper (LNO-214) powders were obtained from commercial suppliers, whilst powders of the double perovskite (GBCO-1125) were prepared by solid state synthesis using the appropriate amounts of $BaCO_3$, Gd_2O_3 and Co_3O_4 precursor oxides. Pellets were made from the powders by pressing uniaxially, followed by isostatic pressing at 300 MPa to aid densification. Samples were placed on a bed of the same powder on alumina plate, covered with more powder and then sintered at 1250 °C for 4 hours (for the single perovskite), 1100 °C for 24 h (double perovskite) and 1300 °C for 10 h (Ruddlesden-Popper). After sintering, all pellets were ground using silicon carbide paper to produce a fresh, flat surface. The single perovskite and double perovskite samples were then further polished with successively finer grades (down to 0.25 μm) of a water-based diamond polishing medium to produce a smooth flat surface.

In order to reveal the surface chemistry of these materials after the high temperature heat treatments required for their application in solid state electrochemical devices, the samples were annealed in a custom built rig, which can be evacuated by turbomolecular pump to a pressure of around 5 x 10^{-7} mbar to minimise the background levels of CO_2 and water vapour which may affect the surface chemistry during the annealing. After evacuation, the annealing tube was backfilled with 200 mbar of dry research grade (99.996%) oxygen. The samples were annealed in this atmosphere for 12 hours at 1000 °C. The temperature ramps for

the heating and cooling of the samples during the annealing was 300 °C h^{-1}, except for GBCO 1125. Due to the high thermal expansion coefficient of this material, [1] we found it necessary to slow cool the sample (150 °Ch^{-1}) after the annealing in order to avoid the formation of cracks at the surface.

Low-Energy Ion Scattering Experiments

The surface composition of the samples was measured by Low Energy Ion Scattering (LEIS) spectroscopy (Qtac^{100}, IonTOF GmbH, Germany).[2] Prior to the analyses, the sample surfaces were exposed to atomic oxygen (at room temperature) in a sample preparation chamber attached to the instrument in order to remove any residual hydrocarbon contaminants after exposure to the atmosphere. The absence of C was confirmed by analysis using 3 keV $^4He^+$ (**Figure S1**), which showed the disappearance of the corresponding peak around 846 eV (theoretical position for $^4He^+$ scattering by ^{12}C). Once this cleaning was complete, a fresh area of the sample surface was selected for the depth profiling measurement.

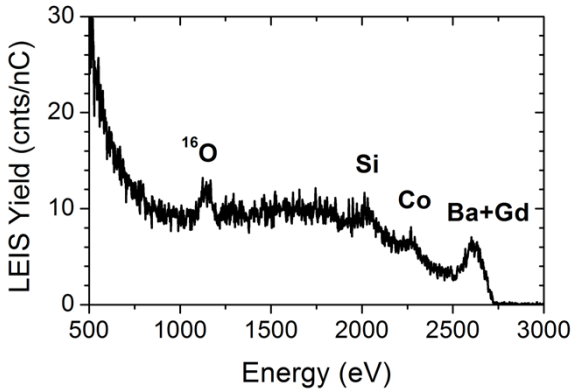

Figure S1 Surface spectrum of the GBCO-1125 sample after polishing obtained with 3 keV $^4He^+$ primary beam.

The depth profiles were acquired using a $^{20}Ne^+$ primary beam (6 keV for the single and double perovskite and 5 keV for the Ruddlesden-Popper samples). The Ne^+ beam gives better separation for heavier masses, allowing us to resolve the peaks for the cations of interest during the depth profiling analyses. The primary ion beam impinges at normal incidence to the sample surface, and primary ions scattered through 145 degrees are collected over the entire azimuth of the detector. Their energy distribution is then measured by a double toroidal energy analyzer. To mitigate any effect of sample charging, the surface was flooded with low energy electrons in a self-regulating charge compensation regime.

In order to ensure the information originated only from the very outer surface of the samples, we were careful to ensure that the primary ion fluence used to acquire each spectrum

remained in the so-called "static regime" (i.e. the product of the sputter yield and primary ion fluence was limited to a few percent of the assumed surface atomic density of 10^{15} atoms cm^{-2}). Assuming typical relative sputter yields of 0.1 at ion^{-1} and 1 at ion^{-1} for $^{4}He^{+}$ and $^{20}Ne^{+}$ in the low-keV energy regime, the ion fluences must be limited to 2 x 10^{14} and 2 x 10^{13} ions cm^{-2} during the analyses with $^{4}He^{+}$ and $^{20}Ne^{+}$, respectively, to satisfy this condition.

In-depth analysis was achieved by sputtering the sample with a 500 eV beam of $^{40}Ar^{+}$ at 59 degrees incidence, interlaced with the ion scattering measurements. To avoid any contribution from the crater side walls to the measured depth profiles, only a region in the centre of the sputtered crater (typically an area of 1000 x 1000 μm^2 centered in a sputtered crater of 1500 x 1500 μm^2) was used for the analysis.

Fitting of LEIS spectra

In order to quantify the spectra, the intensities of various peaks of interest were extracted by fitting using a set of mathematical components, as shown in **Figure S2**. The surface scattering peaks were described by Gaussian peaks, with widths corrected for the isotopic distributions of the surface atoms. The low energy background signals produced by those primary ions which had been scattered below the surface and subsequently re-ionised as they leave the surface were described by error functions. To ensure stable solutions and properly apportion contributions to unresolved peaks (e.g. Ba and Gd), the energy shift between the two (unresolved) background signals was fixed to be the same as the difference between the two surface peak positions.

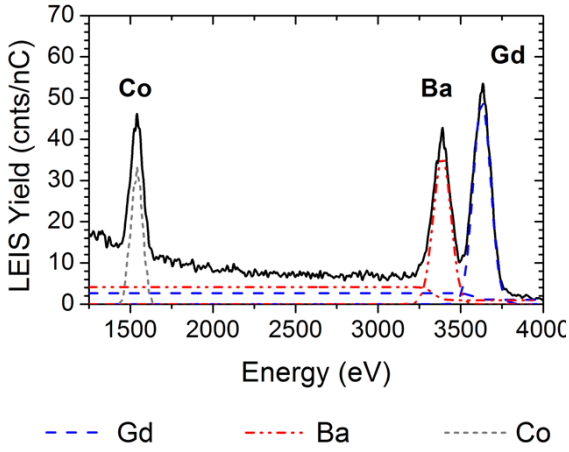

Figure S2 Spectral components used for the fitting of the surface peaks in GBCO-1125. The spectra shown as an example correspond to the bulk composition of the double-perovskite materials after annealing.

Additionally, the LEIS spectra show an exponential signal decay in the low energy range due to the contribution of the atoms sputtered as positive ions from the surface during

the analysis. This effect is larger during the first analysis cycles of the depth profile as a consequence of the presence of hydrocarbons or other contaminants with high positive ionisation probabilities (e.g. H or Na) in the outer layer of the sample surface. No background correction was applied for this contribution in the low energy range. Therefore, it was not possible to use the same fitting components (Gaussian peak + error function) for those atoms appearing in this low energy range (e.g. Co peak in GBCO-1125, **Figure S2**). In this case, the quantification was performed by integrating the area of the peak after subtracting a linear background. The error obtained using this linear background subtraction compared to fitting with a Gaussian peak is less than 3%.

2. Quantification of the compositional depth profiles

The quantification of the fractional cation surface coverage was performed using a similar procedure as the one described by Shin *et al*. [3], and the quantified profiles are shown in **Figure S3**. This procedure assumes that the signal plateau obtained after sufficient sputter fluence corresponds to the nominal bulk cation stoichiometry and allows the quantification of the depth profiles without any need for external standards. The internal calibration applied in this work was show to lead to similar cation surface coverages as the calibration against external standards [3]. Although this methodology leads to a good estimation of the cation coverage on the surface, possible artefacts resulting from ion-solid interactions must be considered in order to avoid any misinterpretation of the results, especially for the first points of the depth profiles.

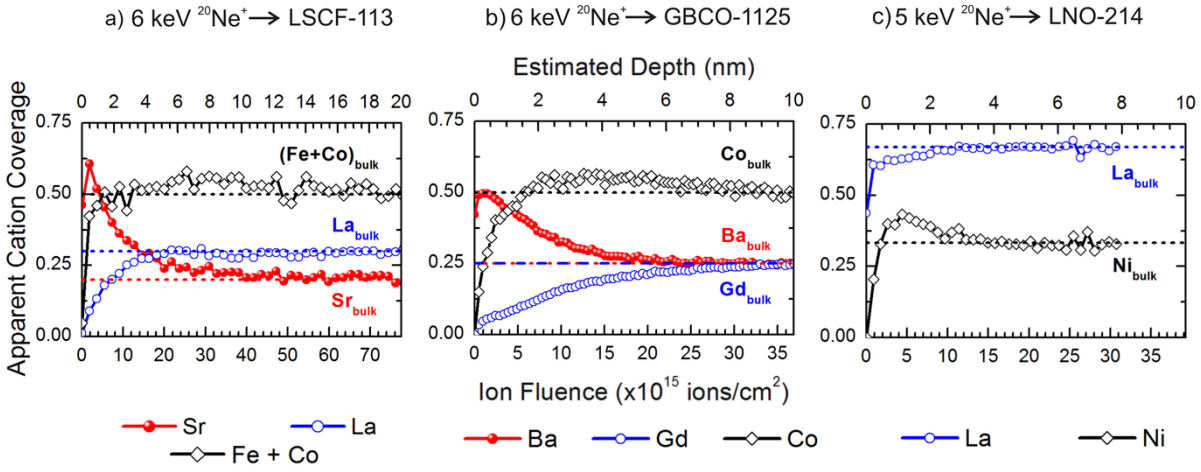

Figure S3 Calibrated LEIS depth profiles showing the apparent cation coverage at the surface and near surface of (a) LSCF-113 perovskite, (b) GBCO-1125 double perovskite and (c) LNO-214 Ruddlesden-Popper samples after being annealed at 1000˚C for 12 hours at pO_2 = 200 mbar. The depth profiles were obtained by low-energy $^{40}Ar^+$ sputtering (@59˚, 500 eV) and the quantification performed according to the method described in the text.

One clear example of the importance of these ion-induced effects is that the cation percentages on the very outer surfaces of the depth profiles (**Figure S3**) do not add up to 100% surface coverage, due to the preferential sputtering of oxygen. As shown in **Table S1**, the sputter yield of oxygen is estimated to be about one order of magnitude higher than the cations under these conditions [4, 5]. Therefore, the total cation coverage of outermost surface appears to be less than 100% due to the higher oxygen content in the surface compared to the bulk coverage values calculated from the plateau signals, when the material is depleted in oxygen.

Sputter Yields (Atoms/Ar^+ ion)					
LSCF		**GBCO**		**LNO**	
La	0.24	**Gd**	0.25	**La**	0.60
Sr	0.45	**Ba**	0.52	**Ni**	0.39
Co	0.11	**Co**	0.59		
Fe	0.44				
O	2.65	**O**	2.30	**O**	2.38
Total	3.89	**Total**	3.66	**Total**	3.37
R_p (Å)	10	**R_p (Å)**	10	**R_p (Å)**	11

Table S 1. Sputtering yields and projected ranges (R_p) obtained by SRIM[4] of the different species present in the perovskite, double-perovskite and Ruddelsden-Popper materials for an 500 eV Ar^+ sputter beam at 59°.

In the same way, the preferential sputtering of the cation species must be also considered. In the case of GBCO-1125 and LSCF-113, the alivalent cations A'= Ba and Sr, respectively, shows a higher sputter yield compared to the A cations, and hence, the A'-enrichment in the outermost surface might be also affected, although its impact is probably much lower than the preferential sputtering of oxygen. Although the preferential sputtering of the A'-cations cannot be ruled out, the difference in the sputter rates are not large enough to lead us to wrong conclusions related to the A'-O surface terminations or the presence of the B-enriched region, which is most likely to be related to the segregation of A and A' cations to the surface rather than to an analysis artefact.

In addition to the effects of ion sputtering, the presence of other species on the outer surface might also have an effect on the estimated cation coverage (e.g. formation of barium carbonates on the GBCO-1125 surface). In order to avoid the formation of these species the

samples were analysed in a short period of time after the polishing and annealing and subsequently cleaned by exposure to the atomic oxygen plasma. The presence of any contamination was checked by the analysis with 3 keV $^4He^+$ beam. For example, Figure S1 shows the He analysis of GBCO-1125 after the polishing. As mentioned above, carbon was not present in any detectable amount, whereas a small trace of Si was detected on the outer surface, but was easily removed after a small amount of sputtering.

3. Depth Calibration

The depth calibration of the profiles was based on the interferometric measurement of the etching rate on a GBCO pellet, since the sputter yields for the three materials are expected to be very similar according to estimates using the "Stopping and Range of Ions in Matter (SRIM)" package (Table S1) [4, 5].

In order to reduce the sputtering time required to obtain a measurable crater on the rough ceramic surface and to avoid variations in the sputter current, the crater area was reduced to 300x300 μm^2. The sputter yield was estimated according to the measured crater depth and the theoretical atomic density as calculated from the lattice parameters. In the case of the GBCO sample, the atomic density is 7.89 x 10^{22} atoms/cm^2 and the measured sputtered yield is 2.0 atoms/incident Ar^+ ion. The sputter rate was assumed to be constant throughout the whole profile, disregarding any change in the sputter yield due to compositional changes due to preferential sputtering of any of the surface species (e.g. oxygen) or any variations in sputter rate during the transient regime.

4. References

1. Zhou, Q., et al., *Performances of $LnBaCo_2O_{5+x}$–$Ce_{0.8}Sm_{0.2}O_{1.9}$ composite cathodes for intermediate-temperature solid oxide fuel cells.* Journal of Power Sources, 2010. **195**(8): p. 2174-2181.
2. Brongersma, H.H., et al., *High-sensitivity and high-resolution low-energy ion scattering.* Vacuum, 2010. **84**(8): p. 1005-1007.
3. Shin, H.H. and S. McIntosh, *On the H_2/D_2 isotopic exchange rate of proton conducting barium cerates and zirconates.* Journal of Materials Chemistry A, 2013. **1**(26): p. 7639-7647.
4. J.F. Ziegler, J.P.B., U. Littmark, *The Stopping and Range of Ions in Solids*. Vol. 1. 1985, New York, US: Pergamon.
5. Ziegler, J.F., M.D. Ziegler, and J.P. Biersack, *SRIM – The stopping and range of ions in matter (2010).* Nuclear Instruments and Methods in Physics Research Section B: Beam Interactions with Materials and Atoms, 2010. **268**(11–12): p. 1818-1823.